JOURNAL OF MATERIALS SCIENCE 26 (1991) 4637–4642

The effect of SiO_2 on high-temperature deformation and strength of zirconia-toughened alumina

A. KRELL, T. REICH, A. BEGER
Zentralinstitut für Festkörperphysik und Werkstofforschung, Helmholtzstr. 20, 0-8027, Dresden, Germany

G. A. GOGOTSI, Y. L. GROUSHEVSKY
Academy of Sciences of the Ukrainian SSR, Institute for Problems of Strength, Kiev, SU 252014, USSR

At room temperature, SiO_2 additions may increase the fracture toughness, K_{Ic}, by diminishing the tetragonal phase contents to about 50%, but with ground surfaces the influence on strength is small. A pronounced decrease in strength is observed with rising temperature in the high toughness region from 20 °C to M_s, the starting temperature for martensitic transformation. Beyond M_s at lower toughness, the strength behaviour is very similar to nontransforming alumina ceramics, and an even modest increase of the silicate concentration intensively promotes propagation-controlled failure in the brittle creep region (> 900 °C) and inelastic deformation. With less than 1% amorphous grain boundary phases, damage-free superplasticity is restricted to small strains of less than 10%. The significance of high-temperature data for tool applications is considered by cutting tests with high feeding rates.

1. Introduction

The toughening effect of the tetragonal–monoclinic phase transformation of ZrO_2 particles dispersed in an alumina matrix has been used for more than 10 years to develop high-strength ceramics [1, 2]. Owing to the increasing stability of the tetragonal phase with rising temperature, the transformation to the monoclinic polymorph becomes more difficult, and the toughening benefit diminishes. Therefore, zirconia-toughened alumina (ZTA) has found engineering application predominantly for use at room temperature with locally occurring heat (tool bits), and little information is available about the mechanical behaviour at high temperatures.

However, for tool bits, temperatures as high as 1000 °C at the cutting edge occur at the same location as the highest mechanical load, and thus investigations of high-temperature deformation mechanisms are of practical importance. Our previous measurements of the hardness of Al_2O_3 and ZTA revealed no differences up to 1300 °C [3]. Cutler *et al.* [4] demonstrated the possibility of strength improvements up to 750 °C (600 MPa) by introducing surface compressive stresses resulting from differing amounts of stabilizing Y_2O_3 in the volume and at the surface of ZTA bars with 15 vol % ZrO_2. In spite of such results, the general understanding of the temperature effect on the mechanical performance of such materials is limited by the narrow scope of the experimental data.

Further interest in the high-temperature behaviour of ZTA arose with the prospect of superplasticity in Al_2O_3 [5], in tetragonal zirconia polycrystals [6], and in ZrO_2 + 20% Al_2O_3 [7], which is possible above 1300 °C even without cavitation damage of the structures. Superplastic flow was reported for high-purity Al_2O_3 obviously containing no continuous amorphous grain-boundary phases, but no data concerning the strength of the deformed parts were given [8].

Often such amorphous phases cannot be avoided using the usual industrial preparation technologies. It was the aim of our present work to investigate the influence of small SiO_2 concentrations on fracture strength and plastic deformability of ZTA up to 1400 °C.

Additionally, we tested to what degree the measured high-temperature properties enable the practical use of the material as a tool for hard cutting conditions. The outstanding performance of ZTA with respect to steel workpieces is well-known and has also been confirmed for our ceramics. Therefore, relating specifically to measured mechanical properties at high temperatures, we shall give here another example, comparing our ZTA with commercially approved hot-pressed and sintered Si_3N_4 tools under cutting conditions that are especially suited for the favourable use of high-strength nitride materials, i.e. the turning of grey cast iron at large feed rates.

2. Experimental procedure

2.1. Materials and their properties at room temperature

Starting with 0.6 μm Al_2O_3 powder (Alcoa A16SG), granules were prepared by adding an aqueous

0022–2461/91 $03.00 + .12

solution of $ZrOCl_2 \cdot 8H_2O$, homogenizing the suspension in a planetary mill for 3 h, drying and calcining at 950 °C for 2 h; the produced mixture contained 16.4 wt % ZrO_2 (about 11.5% by volume) and was again homogenized in the same mill for 10 h with a solution of $MgCl_2 \cdot 6H_2O$ and an organic binder, giving final concentrations of 0.14 wt % MgO and 2 wt % organic acid. The slurry was freeze-dried, bars of dimensions 5 mm × 8 mm × 60 mm were formed by uniaxial pressing at 200 MPa and sintered at 1580 °C for 1 h in hydrogen to a density of at least 97.5% with average grain sizes of 2.2 μm (Al_2O_3) and 1.1 μm (ZrO_2); air sintering produced structures with lower strength due to higher monoclinic phase contents.

Using milling containers and balls made from (A) 99.7% and (B) 96% Al_2O_3, respectively, different structures with about 0.01 and 0.10 wt % SiO_2 were produced. High-voltage and high-resolution electron microscopy revealed little differences between both structures [9]. Most noticeably, with 0.10% SiO_2 there are indications of a higher concentration of larger amorphous triple points and of more grain facets covered by a glassy film. However, even with this raised SiO_2 content, many of the grain boundaries do not contain any trace of secondary phases. Additional Auger investigations confirmed this result (which is contrary to experiences on ZTA prepared by attrition milling routes with 85% Al_2O_3).

Table I gives some properties measured at room temperature. Additionally determined static Young's moduli (Fig. 1, four-point bending) are very close to those measured dynamically (Table I). The fracture toughness, K_{Ic}, was derived from notched beam tests with bars that had been annealed for 1 h at 1350 °C after notching. Dilatometer studies of these ZTA materials showed a starting temperature, M_s, for the tetragonal-to-monoclinic transformation of about 540 °C. Following Table I, SiO_2 destabilizes the tetragonal ZrO_2 polytype and produces a somewhat higher fracture toughness. The origin of the higher monoclinic contents in structure B is presumed to be nucleation promoted by the silicate phase, because amorphous triple points are observed to be preferentially associated with ZrO_2 particles [9]. The similarly high Young's moduli indicate the same low degree of spontaneous microcracking. At relatively high X_m, this gives rise to high residual stresses and the high toughness of Material B. The previously published correlation between K_{Ic} and the density of the microcracks that are generated on macrofracture, revealed

TABLE I Room-temperature properties of investigated ZTA structures

	ρ (g cm^{-3})	X_m	E (GPa)	K_{Ic} (MPa $\sqrt{m}$)	HV (GPa)
A (0.01% SiO_2)	4.10	0.39	364	6.1	17.2
B (0.10% SiO_2)	4.16	0.51	374	8.0	18.0

ρ = density, X_m = monoclinic content of ZrO_2 component (X-ray measurement of unground surfaces using CuK_α), E = Young's modulus, derived from resonance frequency, K_{Ic} = fracture toughness, H_V = Vicker's hardness at 10 kg load.

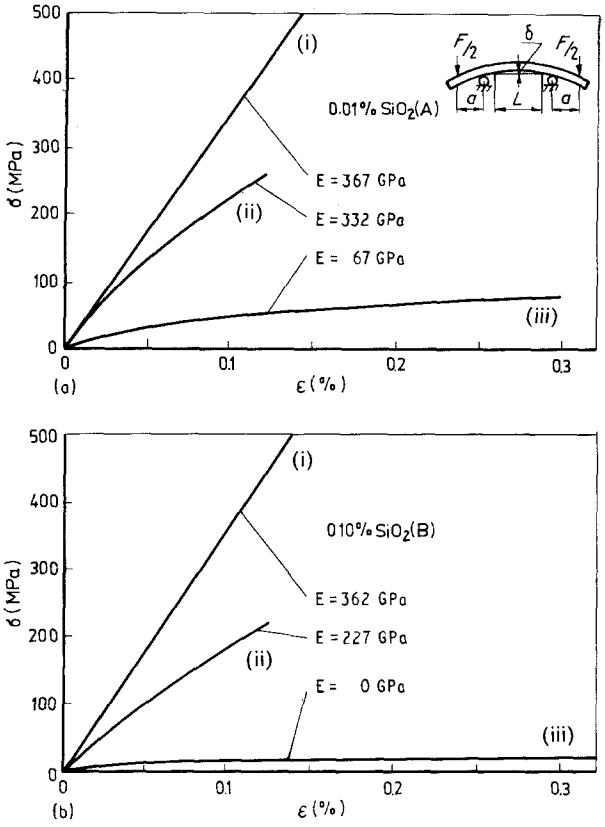

Figure 1 Stress–strain diagrams measured with crosshead velocity 0.5 mm min^{-1} at (i) 20, (ii) 1200 and (iii) 1400 °C. (a) 0.01% SiO_2 (A), (b) 0.10% SiO_2 (B).

microcracking to be the dominating toughening mechanism at room temperature [10]. As a consequence of such energy dissipation [11], in the unground (as-sintered) state, Structure B exhibits a strength improvement of about 15% compared with the purer Material A.

However, before high-temperature testing, the bars had to be ground to dimensions 3.4 mm × 5.0 mm × 50 mm. This was done using a diamond wheel with 100–125 μm grain size, thus encouraging the tetragonal-to-monoclinic transformation in the surface region. As a consequence, X_m rose to more than 0.60, and the resulting compressive stresses are thought to be the reason for the similar room-temperature strengths of both ground materials (Fig. 2), thus overcoming their strength differences measured in the unground state.

With respect to the abrasive wear rate, ZTA A and B are both superior to alumina [12]. The combination of high toughness and hardness of Material B in comparison to Structure A results in a further reduction of wear to 60% [12].

2.2. High-temperature testing methods and cutting experiments

Strength and deformation testing up to 1400 °C in air has been performed using equipment developed at the Kiev Institute [13]. The strength, σ_f, was determined from fracture load, F_f, in three-point bending with span length l = 40 mm and crosshead velocities varying between 0.05 and 5 mm min^{-1}, following the usual

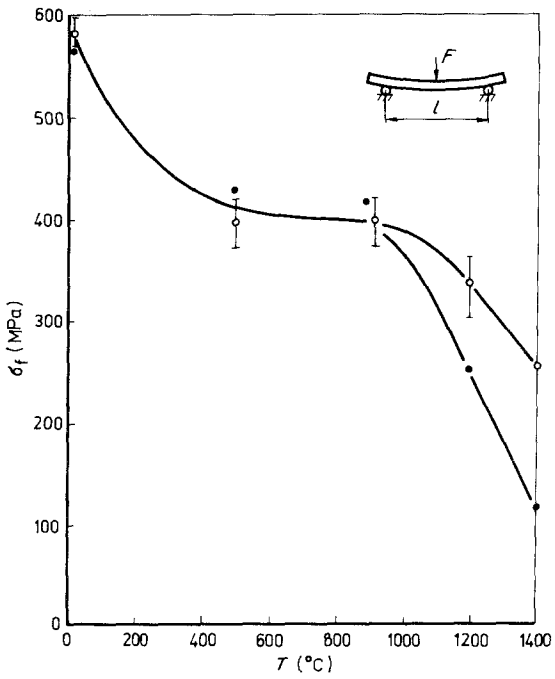

Figure 2 Temperature dependence of the strength of ground ceramics made of Al_2O_3 + 11.5 vol % ZrO_2 (unstabilized). Typical standard deviations are given for Structure B, as an example. (○) 0.01% SiO_2 (A), (●) 0.10% SiO_2 (B).

relationship

$$\sigma_f = \frac{3}{2}\frac{1}{bh^2}F_f \tag{1}$$

where b and h are the specimen width and height, respectively.

In order to obtain accurate deformation data in the elastic as well as in the nonlinear region, special high-temperature experiments in air have been done with a four-point bending assembly. The specimen's stresses, σ, and strains, ε, were recorded by measuring the load, F, dependent deflection, δ [14] using a gauge of length L = 18 mm (Fig. 1)

$$\sigma = \frac{2a}{bh^2}\left(F + \frac{\delta}{2}\frac{dF}{d\delta}\right) \tag{2}$$

$$\varepsilon = \frac{4h}{L^2} \tag{3}$$

(For pure elastic bending $(\delta/2)(dF/d\delta) = F/2$, giving the usual four-point bending stress $3aF/(bh^2)$.) In our experiments, inner and outer span lengths were 20 and 40 mm, so the difference, a, as defined by Fig. 1 was 10 mm. An effective static Young's modulus at high temperatures results as the slope of the stress–strain curves at the origin of the diagram.

Using a similar apparatus but running with vacuum 10^{-2} Pa at the Dresden Institute, we deformed unground (as-sintered) bars of about 3 mm × 6 mm × 50 mm at 1400 °C in bending with a crosshead velocity of 0.05 mm min^{-1}. To produce locally highly strained regions that were to be subjected to subsequent strength testing, the deformation was produced in three-point bending. In the central region of maximum strain, the strain rate was 5×10^{-5} s^{-1}. Then, at room temperature, all pre-deformed bars fractured in their very central part where the plastic deformation was maximum. To compare this bending strength of pre-deformed specimens with that of undeformed bars having the same thermal history, some bars were heated to the same temperature of 1400 °C and cooled without mechanical loading. Fracture stresses of all these specimens were then determined at room temperature in three-point bending with 30 mm span and 0.5 mm min^{-1} crosshead velocity using the relationship [15]

$$\sigma_f = \frac{3F_f l}{2bh^2} + \frac{F_f}{2bh}\frac{\sin\alpha - \mu\cos\alpha}{\cos\alpha + \mu\sin\alpha}\left[6\left(\frac{e}{h} - \frac{1}{2}\right) - 1\right] \tag{4}$$

where μ is the coefficient of sliding friction ($\mu \approx 0.27$ for an unlubricated pair of ZTA/hardened steel [16]), the parameters α and e characterize the degree of pre-deformation and are defined by Fig. 3. With b = 6.5 mm, h = 3.5 mm, $\alpha = 32°$, and e = 6 mm, the correcting term in Equation 4 increases the calculated stress by about 8%. Finally, it should be noted that without plastic deformation the vacuum annealing of unground (B) specimens at 1400 °C/0.5 h enhanced their strength from 555 ± 50 MPa (as-sintered) to 665 ± 65 MPa, an effect which is thought to be analogous to the above advantage of reducing sintering.

Ground quadratic cutting tool inserts (12 mm × 12 mm × 6 mm) with 1 mm nose radius and with 0.3 mm × 20° edge chamfer were produced for tests under the following conditions:

(i) turning lamellar grey cast iron (German code notation GGL 25) with feeding rates of 0.5 and 0.75 mm/rev. at circumferential velocities of 300 and 400 m min^{-1} and a cutting depth of 2 mm;

(ii) turning the same material with interrupted cut (generated by a groove perpendicular to the turning direction) with 0.5 mm/rev. feed and a cutting velocity of 300 m min^{-1}. The depth of cut was again 2 mm.

Under Condition (ii), of course, besides abrasive flank wear, the statistics of microscopic brittle cutting edge failure have to be analysed. However, we observed no significant difference between ZTA and Si_3N_4 tools in

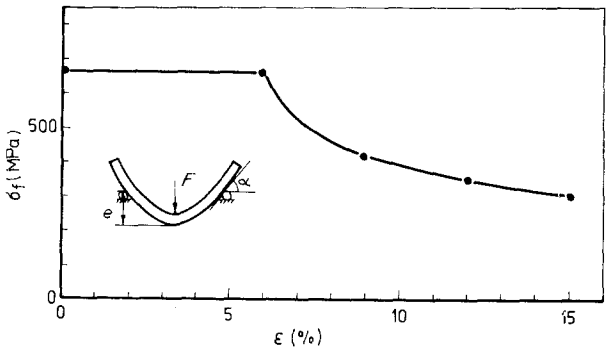

Figure 3 Effect of pre-deformation strain, generated at 1400 °C with 5×10^{-5} s^{-1} in three-point bending, on the room-temperature strength of the unground Material B (0.10% SiO_2). All specimens experienced the same thermal treatment. The given strain is the maximum plastic strain in the centre of the pre-deformed bars.

this respect. Therefore, we shall discuss here only the development of average abrasive flank wear width as monitored by an optical microscope.

3. Results

Fig. 2 gives the temperature dependence of strength for ground specimens with (A) 0.01% and (B) 0.10% SiO_2 when tested with a crosshead velocity, $v_T = 0.5\ mm\ min^{-1}$. As has been observed for alumina [17], we found no effect of v_T on the strength in the range 0.05–5 $mm\ min^{-1}$, even above 1000 °C.

To test the possible influence of grinding-induced surface stresses on the effect of temperature, some ground A-type specimens were heated to 500 °C, cooled and fractured at room temperature. Their average strength was 537 MPa, which is considerably more than the 400 MPa measured at 500 °C (cf. Fig. 2). Therefore, in Fig. 2 the strength loss from room temperature to 500 °C cannot be caused by relaxing surface compressions at this temperature, followed by a simple constancy of structures and properties up to 900 °C. Instead we think that it is necessary to interpret the data in Fig. 2 as a continuous (at first sharp and then becoming flatter) decrease of the intrinsic material strength from room temperature to 900 °C.

Fig. 2 gives thus the usual sequence of changing basic rupture modes with temperature [18]:

(a) brittle rupture with high toughness due to energy dissipative processes (room temperature–500 °C; note that the upper bound of this region meets M_s of the investigated ZTA structures);

(b) brittle rupture with lower toughness and decreasing temperature dependence, both being associated with diminished effectiveness of energy dissipation (500–900 °C),

(c) creep rupture accompanied by a sharp decrease of strength (above 900 °C).

Following Evans and Dalgleish [18], this creep rupture at lower temperatures may occur in a brittle manner; at higher temperatures creep ductility obtains. Deformation diagrams (Fig. 1a, b) indicate a transition from creep brittleness to creep ductility at about 1200 °C, but even at 1400 °C and with 0.10% SiO_2 the fracture surfaces do not reveal any trace of viscous flow or local plastic deformation, nor any difference in the fracture morphologies at 20 and 1400 °C (Fig. 4a, b).

When the crosshead velocity was decreased from 5–0.05 $mm\ min^{-1}$, we observed the usual increasing nonlinearity in the stress–strain diagrams without effect on strength, a known phenomenon discussed previously by Venkateswaran *et al.* [17] which, therefore, we shall not extend here.

With regard to Fig. 4a, b, the nature of the nonlinearity above 900 °C documented in Fig. 1 is extensive macroscopically *inelastic* creep proceeding to *brittle* fracture. In Material B this creep is assisted by the higher contents of amorphous phases in triple points and planar grain boundaries due to the higher SiO_2 concentration. However, though the strain rate of $5 \times 10^{-5}\ s^{-1}$ is usual for superplastic deformation, Fig. 3 reveals that beyond some threshold strain of about 6%, deformation is associated with damage resulting in a decrease of room-temperature strength.

In spite of the ease of high-temperature deformation with 0.10% SiO_2 (Fig. 1b), the strength (Fig. 2) and hardness [3] of B-type ZTA between 20 and 1400 °C are sufficient to enable the preparation of high-performance cutting tools (Fig. 5). Whereas for mild abrasive conditions the reduced wear of Composition B at room temperature had been recognized previously [12], Fig. 5 documents small wear for tools at high feed rates. It should be emphasized that the results of Fig. 5 are not biased by an unsatisfactoring performance of the Si_3N_4 reference materials, because the testing conditions chosen are especially favourable for Si_3N_4 tools. For uninterrupted turning with higher feed of 0.75 mm rev., 300 $m\ min^{-1}$ velocity and 2 mm depth of cut, the ratios between the tested tool materials are the same ones as in Fig. 5. Experiments with 1 min cutting time at increasing feed always showed lower wear of ZTA in uninterrupted and interrupted tests (1 and 4 grooves) up to 1 mm/rev. However, ZTA was fractured at about 1.1–1.3 mm/rev., whereas Si_3N_4 tools were tested at 1.5 mm/rev. without rupture.

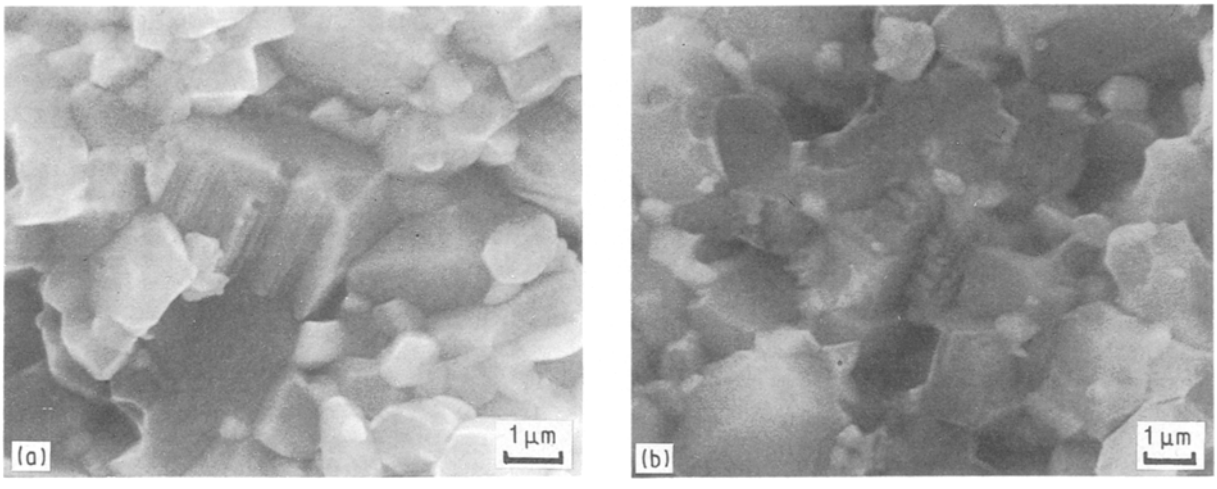

Figure 4 Scanning electron micrographs of fracture surfaces of Structure B (0.10% SiO_2) ruptured at (a) 20 °C, and (b) 1400 °C, respectively.

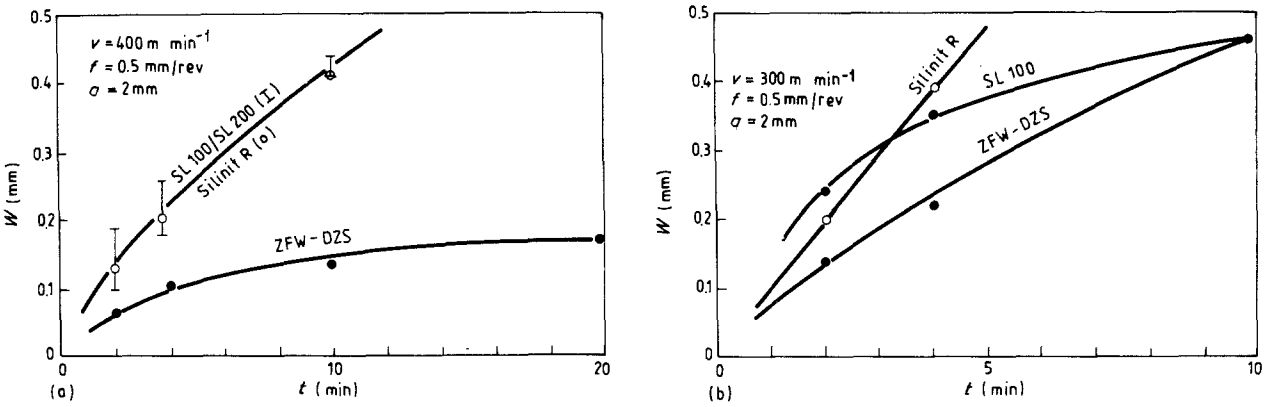

Figure 5 Average width of flank wear for (a) continuous and (b) interrupted cutting of grey cast iron with large feeding rates, f (v = circumferential cutting velocity, a = depth of cut); no coolant fluid used. SL100 and SL200 (same results for both kinds of tools) are commercial Si_3N_4 tools, as is Silinit R, which is hot-pressed Si_3N_4/TiN. ZFW-DZS is the Al_2O_3/ZrO_2 Material B investigated here (0.10% SiO_2).

4. Discussion

The main driving force of the martensitic transformation, the free energy difference between tetragonal and monoclinic ZrO_2, depends on temperature as a linear function. Following Lange [19], in ZTA from room temperature to M_s (here about 540 °C) this causes a linear drop of K_{Ic} and a similar temperature dependence of strength. However, this simple relationship requires a constant transformable amount of tetragonal particles over the investigated temperature range: if, at rising $T < M_s$, spontaneous retransformation to tetragonal symmetry supplies an increasing content of such particles which, in a stressed fracturing part, can again undergo a transformation to the monoclinic polytype, then, inversely, the toughness may be increased with increasing temperature [20]. Yet another influence arises from microcrack toughening around transformed, monoclinic grains – an effect that diminishes with increasing temperature due to the diminishing monoclinic contents.

It is, therefore, not surprising that a simple linear relationship is not observed and that different ZTA structures with their varying ratios between those influences exhibit rather different degrees of strength deterioration from 20 °C to M_s. For example, the convex curvature in Fig. 2 up to 900 °C has the same character as observed by Cutler *et al.* [4] for another (but unground) ZTA with unstabilized zirconia, whereas high additional surface compressions originating from a gradient of stabilizer (Y_2O_3) concentration in the same temperature range were associated with a concave shape of the strength decrease, and a linear relationship was observed for a usual $Al_2O_3/ZrO_2(Y_2O_3)$ composite [4].

It must thus be concluded that due to the different importance of competing mechanisms in various ZTA ceramics, no unit character of strength degradation up to M_s exists.

Beyond M_s the investigated zirconia-toughened ceramics show a common modest strength decrease as nontransforming Al_2O_3 or Al_2O_3/TiC materials as a consequence of increasing stress corrosion. This occurs on the same stress level of about 400 MPa which is characteristic for those structures. This similarity implies that for ZTA above M_s the effect of transformation toughening is really already rather small, procuring no more than the uniform course of the σ–T curve around M_s.

Macroscopic plastic deformation due to dislocation activity at 1400 °C or even below has been observed in single crystals as well as in sintered polycrystals of Al_2O_3 [21–23] and of tetragonal ZrO_2 [6, 24]. However, up to 1600 °C, possible macroscopic deformation rates for sapphire are smaller than $10^{-5}\,s^{-1}$ [25, 26]; with cubic ZrO_2 single crystals, it is $10^{-3}\,s^{-1}$ at 1500 °C, but only for special crystallographic orientations [27]. This and the fairly small content of 11.5 vol % ZrO_2 explain the pure brittle character of ZTA fracture surfaces produced at 1400 °C (Fig. 4b). Therefore, beyond 900 °C the different degrees of strength deterioration (Fig. 2) and plasticity (Fig. 1) with 0.01% and 0.10% SiO_2 have to be understood as grain-boundary creep processes.

Keeping in mind the crystal brittleness, to a first approximation the stress state at the tip of some main flaw at 1400 °C should be similar to the pure elastic fields at lower temperatures. We thus expect the stress concentration at the crack tip to produce damage, especially in the form of cavitations at triple points. Of course, such damage will be favoured by amorphous heterogeneities, and in fact silicon-containing localized regions of amorphous phases have been observed to act as crack nucleation sites in Al_2O_3 [28, 29]. On the other hand, it has been argued that such damage-controlled failure should be prevalent at low crack growth rates only ($< 1\,\mu m\,s^{-1}$) [18]. Following Evans and Dalgleish [18], for ceramics without a continuous amorphous grain-boundary phase, the observed strength loss in the brittle creep region (Fig. 2, beyond 900 °C) is dominated by subcritical crack propagation-controlled failure, by some direct, relatively fast extension mechanism ($> 10\,\mu m\,s^{-1}$) including short-range diffusion and viscous flow at narrow crack tips; with a wetting fluid present, the geometrical condition of a narrow crack can also hold at lower velocities. Although the corresponding visco-elastic behaviour pertinent to fine-grained polycrystals has yet to be evaluated, the promoting effect of amorph-

ous phases, even in the situation of discontinuous distribution, on diffusion and matter deposition is obvious.

Figs 1 and 3 demonstrate the ease of plastic deformation at 1400 °C under a low stressing load of about 15 MPa and a strain rate of $5 \times 10^{-5}\ s^{-1}$, which is common for superplastic procedures. Nevertheless, when some threshold strain is exceeded, strength-reducing damage cannot be avoided in Structure B (0.10% SiO_2). Obviously, the absence of a continuous amorphous grain-boundary phase does not only not prevent the strength loss above 900 °C associated with subcritical stress corrosion; rather microdamage at low crack velocity (e.g. increasing with strain grain-boundary cavitation [30, 31]) supplies additional promotion for subcritical crack growth at high temperature [18], and after cooling causes a strength loss of pre-deformed specimens at room temperature. We suppose that the existence of a threshold strain of about 6% is associated with the only limited, discontinuous occurrence of amorphous grain-boundary films in this structure. Although easy deformation in Al_2O_3-base ceramics is possible with a glass content of less than 1% (Fig. 1), suppression of cavitation and of shear-band localization of the deformation are prerequisites for damage-free superplasticity and, obviously, require higher concentrations of amorphous phases. TEM investigations have been started to investigate further the effect of glass content on the nature of strain-induced damage.

On the other hand, a content of 0.10% SiO_2 and the associated occurrence of heterogeneously distributed amorphous and "clean" grain boundaries, avoid a deterioration of wear resistance under conditions of high feed rates in continuous and in interrupted cutting.

5. Conclusions

Zirconia-toughened aluminas exhibit three temperature regions of strength. Between room temperature and about 900 °C the strength decreases to a degree that depends on the temperature-dependent toughening ratio between competing mechanisms such as transformation toughening, microcrack toughening, stress corrosion, whereas the effect of temperature on strength is rather strong between room temperature and M_s, from M_s to 900 °C ZTA shows a stress level and a temperature dependence similar to those observed for Al_2O_3. Above 900 °C an excessive strength deterioration occurs in the region of brittle creep rupture, presumably by a visco-elastic mechanism of direct subcritical crack growth. Amorphous phases promote such processes and may act as crack nucleation sites at lower crack growth rates, even if their concentration is low and if localized amorphous regions are separated by "pure" grain boundaries.

Nevertheless, the material with 0.10% SiO_2 has been successfully used for tool applications not only for turning steel, but also for continuous and interrupted cutting of grey cast iron with high feed rates. This behaviour points to the surprisingly small importance of the rather low macroscopic strength beyond M_s for such applications.

Superplastic flow at low deformation rates and small stresses of about 15 MPa is possible at 1400 °C. It is promoted by amorphous phases but does not generally need a continuous distribution of glassy films over a majority of grain boundaries. However, damage-free generation of large strains beyond 6% obviously requires more than about 0.1%–0.3% amorphous grain-boundary phase.

Acknowledgement

The authors gratefully acknowledge the cooperation of Dr P. Blank who prepared the ZTA specimens.

References

1. N. CLAUSSEN, *Z. Werkstoff.* **13** (1982) 138.
2. *Idem., ibid.* **13** (1982) 185.
3. A. KRELL and O. V. BAKUN, *Acta Metall.* **34** (1986) 1315.
4. R. A. CUTLER, J. D. BRIGHT, A. V. VIRKAR and D. K. SHETTY, *J. Amer. Ceram. Soc.* **70** (1987) 714.
5. C. CARRY and A. MOCELLIN, *Proc. Brit. Ceram. Soc.* **33** (1983) 101.
6. R. DUCLOS and J. CRAMPON, *J. Mater. Sci. Lett.* **6** (1987) 905.
7. F. WAKAI and S. KANZAKI, German Pat. DE-3610528, published in group C 04 B 35/48 (1986).
8. K. R. VENKATACHARI and R. RAJ, *J. Amer. Ceram. Soc.* **69** (1986) 135.
9. E. PIPPEL and J. WOLTERSDORF, *Phil. Mag. A* **56** (1987) 595.
10. A. KRELL, P. BLANK and T. WEISS, *J. Mater. Sci.* **22** (1987) 3304.
11. W. POMPE and W. KREHER, in "Advances in Ceramics", Vol. 12, edited by N. Claussen, M. Rühle and A. H. Heuer (The American Ceramic Society, Columbus, OH, 1983), p. 283.
12. A. KRELL and P. BLANK, *Wear* **124** (1988) 327.
13. G. A. GOGOTSI, YA. L. GROUSHEVSKY and V. P. ZAVADA, *Ogneupory* (1988) 33.
14. G. A. GOGOTSI, YA. L. GROUSHEVSKY, V. P. ZAVADA and A. N. NEGOVSKY, *ibid.* (1988) 23.
15. H. BALKE, unpublished research report, ZFW Dresden (1988).
16. T. A. LIBSCH, P. C. BECKER and S. K. RHEE, *Wear* **110** (1986) 263.
17. A. VENKATESWARAN, K. Y. DONALDSON and D. P. H. HASSELMAN, *J. Amer. Ceram. Soc.* **71** (1988) 565.
18. A. G. EVANS and B. J. DALGLEISH, in "Creep and Fracture of Engineering Materials", edited by B. Wilshire and R. W. Evans (The Institute of Metals, London, 1987) p. 929.
19. F. F. LANGE, *J. Mater. Sci.* **17** (1982) 255.
20. P. F. BECHER, M. V. SWAIN and M. K. FERBER, *ibid.* **22** (1987) 76.
21. M. L. KRONBERG, *J. Amer. Ceram. Soc.* **45** (1962) 274.
22. P. F. BECHER, *J. Mater. Sci.* **6** (1971) 275.
23. E. PASSMORE, A. MOSCHETTI and T. VASILOS, *Phil. Mag.* **13** (1966) 1157.
24. R. A. LANKFORD, J. LANKFORD and S. SPOONER, *J. Mater. Sci.* **19** (1984) 3360.
25. D. J. GOOCH and G. W. GROVES, *ibid.* **8** (1973) 1238.
26. *Idem., Phil. Mag.* **28** (1973) 623.
27. R. P. INGEL, D. LEWIS, B. A. BENDER and R. W. RICE, *J. Amer. Ceram. Soc.* **65** (1982) C150.
28. B. J. DALGLEISH, S. M. JOHNSON and A. G. EVANS, *ibid.* **67** (1984) 741.
29. S. M. JOHNSON, B. J. DALGLEISH and A. G. EVANS, *ibid.* **67** (1984) 759.
30. A. G. EVANS, J. R. RICE and J. P. HIRTH, *ibid.* **63** (1980) 368.
31. R. A. PAGE, J. LANKFORD, K. S. CHAN, K. HARDMAN-RHYNE and S. SPOONER, *ibid.* **70** (1987) 137.

Received 2 May
and accepted 29 September 1989